nature microbiology

ARTICLES

PUBLISHED: 26 SEPTEMBER 2016 | ARTICLE NUMBER: 16167 | DOI: 10.1038/NMICROBIOL.2016.167

Root-hair endophyte stacking in finger millet creates a physicochemical barrier to trap the fungal pathogen *Fusarium graminearum*

Walaa K. Mousa[1,2], Charles Shearer[1], Victor Limay-Rios[3], Cassie L. Ettinger[4], Jonathan A. Eisen[4] and Manish N. Raizada[1]*

The ancient African crop, finger millet, has broad resistance to pathogens including the toxigenic fungus *Fusarium graminearum*. Here, we report the discovery of a novel plant defence mechanism resulting from an unusual symbiosis between finger millet and a root-inhabiting bacterial endophyte, M6 (*Enterobacter* sp.). Seed-coated M6 swarms towards root-invading *Fusarium* and is associated with the growth of root hairs, which then bend parallel to the root axis, subsequently forming biofilm-mediated microcolonies, resulting in a remarkable, multilayer root-hair endophyte stack (RHESt). The RHESt results in a physical barrier that prevents entry and/or traps *F. graminearum*, which is then killed. M6 thus creates its own specialized killing microhabitat. Tn5-mutagenesis shows that M6 killing requires c-di-GMP-dependent signalling, diverse fungicides and resistance to a *Fusarium*-derived antibiotic. Further molecular evidence suggests long-term host–endophyte–pathogen co-evolution. The end result of this remarkable symbiosis is reduced deoxynivalenol mycotoxin, potentially benefiting millions of subsistence farmers and livestock. Further results suggest that the anti-*Fusarium* activity of M6 may be transferable to maize and wheat. RHESt demonstrates the value of exploring ancient, orphan crop microbiomes.

Finger millet (*Eleusine coracana*) is a cereal crop grown by subsistence farmers in Africa and South Asia[1,2]. It was domesticated in East Africa around 5000 BC, reaching India by 3000 BC (ref. 3). Subsistence farmers report that finger millet is widely resistant to pathogens including *Fusarium* species[4,5]. One species, *F. graminearum*, causes devastating diseases in crops related to finger millet, including maize and wheat, associated with accumulation of the mycotoxin deoxynivalenol (DON), which affects humans and livestock[6,7]. Despite its prevalence across cereals, curiously, *F. graminearum* is not an important pathogen of finger millet[4,8].

The resistance of finger millet grain to fungal disease has been attributed to high polyphenol concentrations[9,10]. However, the emerging literature suggests that microbes that inhabit plants without themselves causing disease, defined as endophytes, may contribute to host resistance against fungal pathogens[11,12]. Endophytes suppress diseases through the induction of host resistance genes[13], competition[14] and/or the production of antipathogenic compounds[15,16].

Fusarium species date to >8.8 million years ago, and their diversification appears to have co-occurred with the C4 grasses (including finger millet), certainly pre-dating finger millet domestication in Africa[17]. Multiple studies have reported the presence of *Fusarium* in finger millet in Africa and India[18–23]. *F. verticillioides* (synonym *F. moniliforme*) has been observed in finger millet in Africa, and it has been suggested that the species evolved there[18]. These observations suggest the possibility of co-evolution within finger millet of *Fusarium* and millet endophytes. We previously isolated fungal endophytes from finger millet and showed that their natural products have anti-*Fusarium* activity[4]. We could not find reports of bacterial endophytes isolated from finger millet.

The objectives of this study were to isolate bacterial endophytes from finger millet, assay for anti-*Fusarium* activity, and characterize the underlying mechanisms at the cellular, biochemical and molecular levels. We report an unusual symbiosis between the host and a root-inhabiting bacterial endophyte.

Results

Isolation, identification and antifungal activity of endophytes. Seven bacterial endophytes (strains M1–M7) were isolated from surface-sterilized finger millet tissues (Fig. 1a,b and Supplementary Table 1). 16S rDNA BLAST and phylogenetic analyses (Supplementary Fig. 1) identified them as *Enterobacter* (M1, M6), *Pantoea* (M2, M4) and *Burkholderia* species (M3, M5, M7) (GenBank accession numbers for M1–M7: KU307449–KU307455). Interestingly, five of the seven strains showed antifungal activity against *F. graminearum in vitro* (Fig. 1c,d). Strain M6 from millet roots was the most potent and was thus selected for further study, including electron microscopy (elongated, wrinkled surface, Fig. 1e) and whole-genome sequencing, resulting in a final taxonomic classification (*Enterobacter* sp., strain UCD-UG_FMILLET)[24]. M6 inhibited 5 of 20 additional crop-associated fungi, including pathogens, suggesting a wider target spectrum (Supplementary Table 2). Following seed coating, green fluorescent protein (GFP)-tagged M6 localized to millet roots intercellularly and intracellularly (Fig. 1f,g), but did not cause pathogenic symptoms (Supplementary Fig. 2), confirming that M6 is an endophyte of finger millet.

To determine whether M6 has anti-*F. graminearum* activity *in planta*, related *Fusarium*-susceptible cereals (maize, wheat) were used (Fig. 1h–r), given the reported tolerance of finger millet. Seed-coated GFP-tagged M6 colonized the internal tissues of maize (Fig. 1h) and wheat (Fig. 1n). Treatments with M6 (combined seed

[1]Department of Plant Agriculture, University of Guelph, Guelph, Ontario N1G 2W1, Canada. [2]Department of Pharmacognosy, Mansoura University, Mansoura, Egypt. [3]Department of Plant Agriculture, University of Guelph, Ridgetown Campus, Ridgetown, Ontario N0P 2C0, Canada. [4]University of California Davis Genome Center, Davis, California 95616, USA. *e-mail: raizada@uoguelph.ca

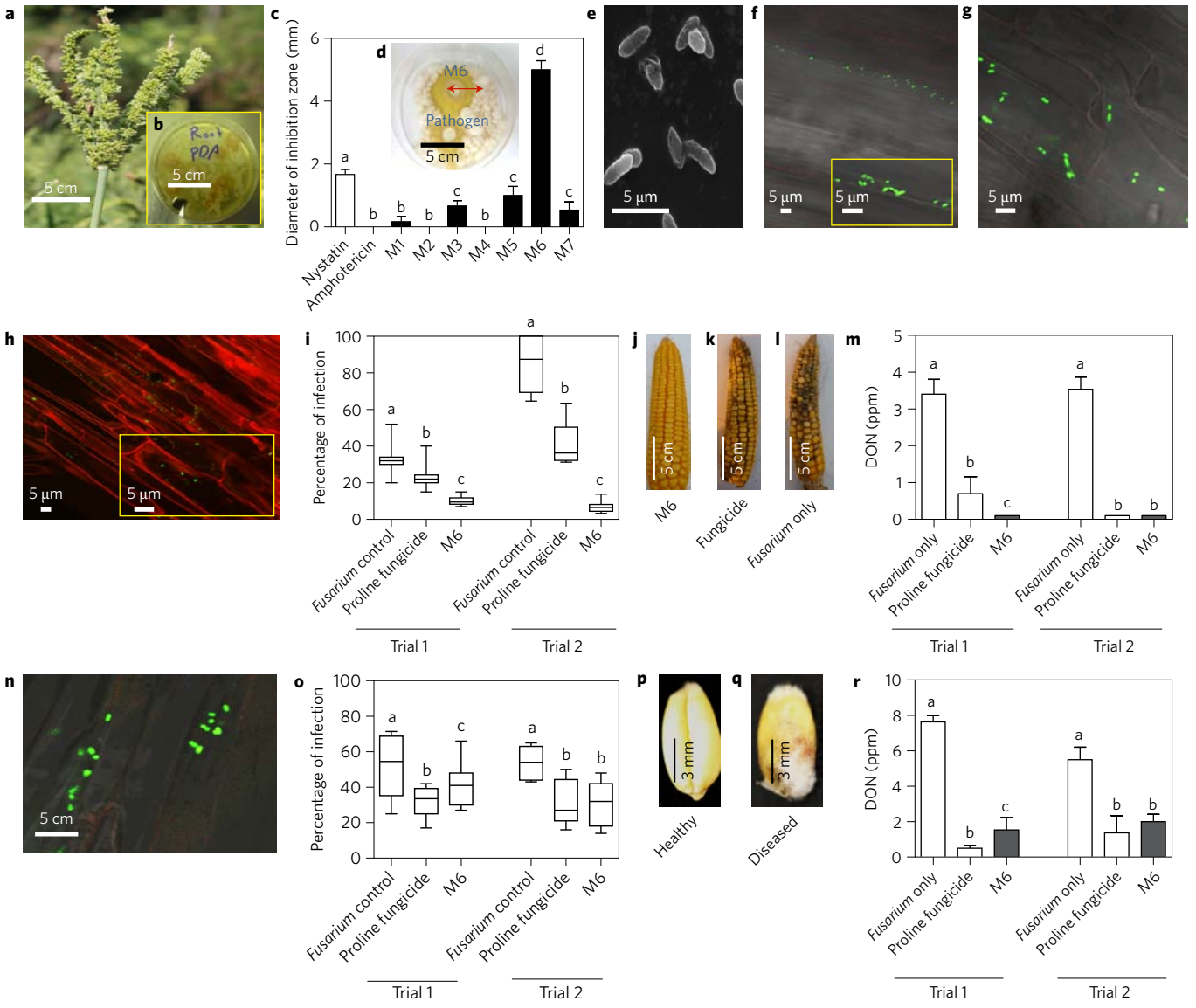

Figure 1 | Isolation, identification and antifungal activity of endophytes. a, Photograph of a finger millet grain head. **b**, Mixed culture of endophytes isolated from finger millet. **c**, Quantification of the inhibitory effect of finger millet endophytes or fungicide controls on the growth of *F. graminearum in vitro*. For these experiments, $n = 3$ biological replicates. **d**, M6 endophyte suppresses the growth of *F. graminearum* hyphae (white) using the dual culture method. **e**, SEM image of M6. **f**,**g**, GFP-tagged M6 inside roots of finger millet viewed by scanning confocal microscopy. **h**–**m**, M6 bioassays in maize: GFP-tagged M6 inside roots of maize (stained with propidium iodide) (**h**); effect of M6 treatment on suppression of *F. graminearum* disease in maize in two greenhouse trials (**i**); representative ears from M6, fungicide and *Fusarium* only treatments (**j**–**l**, left to right); effect of M6 or controls on reducing DON mycotoxin contamination in maize during storage following the two greenhouse trials (**m**). **n**–**r**, M6 bioassays in wheat: GFP-tagged M6 inside roots of wheat viewed by confocal microscopy (**n**); effect of M6 treatment on suppression of *F. graminearum* disease in wheat in two greenhouse trials (**o**); image of a healthy wheat grain (**p**); picture of an infected wheat grain (**q**); effect of M6 or controls on reducing DON mycotoxin contamination in wheat during storage following the two greenhouse trials (**r**). Error bars in **c**, **m** and **r**, indicate standard error of the mean. Whiskers in **i** and **o** indicate the range of data points. For greenhouse disease trials, $n = 20$ biological replicates for M6 and $n = 10$ for controls. For DON quantification, $n = 3$ biological replicate pools of seeds. For all graphs, letters that are different from one another indicate that their means are statistically different using Mann–Whitney *t*-tests ($P \leq 0.05$). Images are representative of ≥3 biological replicates (**d**–**h**,**n**), ≥10 biological replicates (**j**–**l**) or >1,000 biological replicates (**p**,**q**).

coating and foliar spray) caused significant ($P \leq 0.05$) reductions in *F. graminearum* disease symptoms in maize (Gibberella ear rot, Fig. 1i–l) and wheat (Fusarium head blight, Fig. 1o–q), ranging from 70 to 92% and 21 to 43%, respectively, compared to plants treated with *Fusarium* only, in two greenhouse trials (for yield data see Supplementary Fig. 3 and Supplementary Table 3). Following incomplete drying and extended storage to mimic the conditions of African subsistence farmers (ambient temperature and moisture), M6 treatments resulted in dramatic reductions in DON, with levels declining by 97% and up to 81% in maize and wheat, respectively, compared to plants treated with *Fusarium* only, at $P \leq 0.05$ (Fig. 1m,r; Supplementary Table 4).

Microscopic imaging of M6–*Fusarium* interactions in millet roots and *in vitro*. Because *F. graminearum* infects cereal roots[25] and M6 is root-derived, finger millet roots were selected to visualize interactions between M6 and *F. graminearum* (Fig. 2). GFP-tagged M6 was coated onto millet seed. Following germination (Fig. 2a), GFP–M6 showed a sporadic, low-titre distribution throughout the seminal roots (Fig. 2b). Following inoculation with *F. graminearum*,

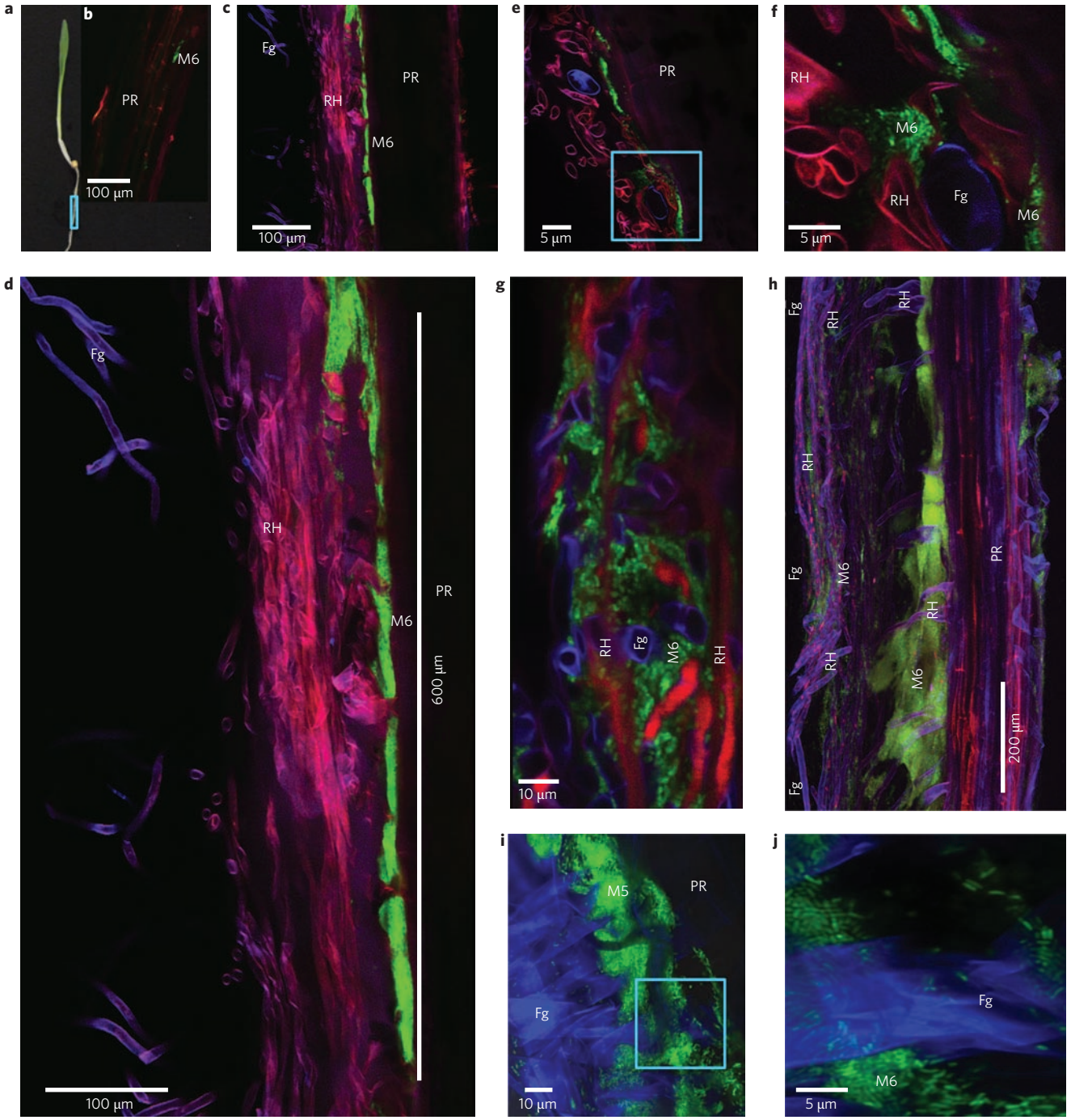

Figure 2 | Confocal imaging of M6–*Fusarium* interactions in finger millet roots. a, Image of millet seedling showing the primary root (PR) zone used for confocal microscopy. **b**, Control primary root that was seed coated with GFP–M6 (green) but not infected with *F. graminearum*. As a control, the tissue was stained with fungal stain Calcofluor to exclude the presence of other fungi. **c**–**h**, Root following seed coating with GFP-tagged endophyte M6 (M6, green) following inoculation with *F. graminearum* (Fg, purple blue, Calcofluor stained) showing interactions with root hairs (RH, magenta, lignin autofluoresence). **c**,**d**, Low (**c**) and high (**d**) magnifications to show the dense root hair and endophyte barrier layers. **e**,**f**, Low (**e**) and high (**f**) magnifications at the edge of the barrier layers. **g**, High magnification in a deeper confocal plane of the root hair layer shown in **d**, showing root hair endophyte stacking (RHESt) with trapped fungal hyphae. **h**, A 62 µm confocal stack with 46 sections showing the multiple features associated with RHESt. *Fusarium* hyphae were visible ~1 mm to the left of the developing RHESt, but hyphae within the image may have already been killed or obscured (see also Supplementary Video 1). **i**,**j**, Low (**i**) and high (**j**) magnifications of the interactions between M6 (green) and *F. graminearum* in the absence of root hair–lignin autofluorescence, showing breakage of fungal hyphae. Pictures are representative of ≥3 biological replicates.

visualized using Calcofluor (Sigma-Aldrich), GFP–M6 accumulated at sites of attempted *Fusarium* entry, creating a remarkable, high-density layer of microcolonies along the entire root epidermal surface—the rhizoplane (Fig. 2c,d). External to the M6 barrier was a thick mat of root hairs (Fig. 2c,d, RH). Root hair number and length were much greater at sites of M6 accumulation than at the opposite side (Fig. 2c), and M6 produced auxin (a known RH-growth-promoting plant hormone) *in vitro* (Supplementary Fig. 4)[26]. Interestingly,

most root hairs were bent, parallel to the root axis (Fig. 2d). The root-hair mat obscured M6, but in an area of low root hair density (Fig. 2e), M6 cells were clearly visible, appearing to attach onto root hairs and engulf *Fusarium* hyphae (Fig. 2f). Imaging at deeper confocal planes (Fig. 2g) revealed that M6 cells were intercalated between bent root hairs, forming an unusual, multilayer root hair–endophyte stack (RHESt) that trapped *F. graminearum* within.

In a subsequent independent experiment, the multiple lines of defence associated with RHESt (rhizoplane barrier, elongated root hairs, root hair intercalations) were captured in a single image by stacking 46 confocal sections (62 μm; Fig. 2h). In this image, *F. graminearum* was inoculated only from one side (the left). *Fusarium* hyphae were visible at a distance (~1 mm) from the developing RHESt, but closer hyphae may have already been killed or are obscured. The stack was rendered into a three-dimensional video (Supplementary Video 1).

In instances where *F. graminearum* was in close contact with the root system, *Fusarium* hyphae became trapped within the RHESt (Fig. 2g). By imaging only the M6–*Fusarium* interaction, hyphal breakage was observed within the RHESt (Fig. 2i,j). To confirm that M6 actively kills *Fusarium*, Evans blue vitality stain, which stains dead hyphae blue, was used following co-incubation on a microscope slide. Hyphae in contact with M6 stained blue and appeared broken (Fig. 3a), in contrast to the control (*F. graminearum* exposed to buffer, Fig. 3b), but similar to the commercial biofungicide, *Bacillus subtilis* (Fig. 3c). These results suggest that M6 cooperates with root-hair cells to create a specialized killing microhabitat (RHESt) that protects millet roots from *F. graminearum* invasion.

Because M6 was sporadically localized in roots in the absence of *Fusarium*, but accumulated at or near sites of *Fusarium*, we hypothesized that M6 actively seeks *Fusarium*. To test this, GFP-tagged M6 and *F. graminearum* were adjacently spotted on an agar-coated slide. As time progressed, M6 swarmed towards *Fusarium* (Fig. 3d–i), confirming its seeking ability. M6 cells then physically attached onto *Fusarium* hyphae (Fig. 3g–i), then dense M6-microcolonies cleaved the hyphae (Fig. 3j). This motility was enabled by multiple peritrichous flagella (Fig. 3k). As this interaction was observed *in vitro*, independent of the host, M6 alone appears sufficient to exert its fungicidal activity. To test whether M6 adhesion is mediated by biofilm, scanning electron microscopy (SEM) was used, which showed biofilm matrix formation associated with M6 cells *in vitro* (Fig. 3l). Biofilm formation was confirmed independently using the proteinaceous biofilm stain, Ruby Film Tracer (red; Fig. 3m and Supplementary Video 2).

Combined, these results suggest that M6 cells swarm towards *Fusarium* hyphae attempting to penetrate the root epidermis, associate with induced root-hair growth and bending, which results in the formation of RHESt, within which M6 cells form biofilm-mediated microcolonies that attach, engulf and kill *Fusarium*.

Identification of M6 genes required for anti-*Fusarium* activity. Because M6 could exert fungicidal activity without millet, it was feasible to screen Tn5-mutagenized M6 *in vitro* for loss of activity against *F. graminearum*. Of 4,800 insertions (screened in triplicate), 16 mutants resulted in reduced/lost inhibition of *F. graminearum* (Supplementary Fig. 5a). Complete loss-of-function mutants were validated *in planta* in replicated greenhouse trials using maize (Supplementary Fig. 5b,c), demonstrating the relevance of the *in vitro* results. BLAST searching of rescued Tn5-flanking sequences against the wild-type M6 genome[24] identified 13 candidate genes in 12 predicted operons (Supplementary Tables 5 and 6). Based on gene annotations and published reports, four regulatory and/or antimicrobial mutants of interest were selected, complemented (Supplementary Fig. 5d) and characterized. The selected genes encode: (1) the LysR transcription regulator in a phenazine operon (*ewp*R-5D7::Tn5), (2) the LysR transcriptional regulator in a FA resistance operon (*ewf*R-7D5::Tn5), (3) diguanylate cyclase (*ewg*S-10A8::Tn5) and (4) a colicin V production protein (*ewv*C-4B9::Tn5).

LysR transcription regulator in a phenazine operon (*ewp*R-5D7::Tn5). *ewp*R-5D7::Tn5 resulted in complete loss of the antifungal activity *in vitro* (Supplementary Fig. 5a) and reduced activity *in planta* (Fig. 4a). Tn5 inserted in an operon (*ewp*, Fig. 4b) that included tandem paralogues of *phz*F (*ewp*F1, *ewp*F2) (*trans*-2,3-dihydro-3-hydroxyanthranilate isomerase, EC #5.3.3.17), a homodimer enzyme that synthesizes the core skeleton of phenazine (Fig. 4c), a potent fungicide[27]. Tn5 specifically inserted within a member of the LysR transcriptional regulator family (*ewp*R), previously reported to induce phenazine biosynthesis[28]. LysR was transcribed in the opposite direction as the operon. The LysR canonical binding site sequence ($TN_{11}A$)[29] was observed upstream of the *phz*F (*ewa*F) coding sequences (Fig. 4b). Real-time PCR revealed that the expression of *ewp*F1 and *ewp*F2 was dramatically downregulated in the LysR mutant compared to wild type (Fig. 4d). Combined, these three results suggest that EwpR is a regulator of phenazine biosynthesis in M6. The crude methanolic extract from *ewpR*-5D7::Tn5 lost anti-*Fusarium* activity *in vitro*, in contrast to extracts from wild-type M6 or randomly selected Tn5 insertions that otherwise had normal growth rates (Fig. 4e). Anti-*F. graminearum* bioassay-guided fractionation using M6 extracts showed two active fractions (FrA, FrB) (Fig. 4e–g), each containing a compound with a diagnostic fragmentation pattern ($[M+H]^+ = 181.0$), corresponding to a phenazine nucleus ($C_{12}H_8N_2$, $M_w = 180.08$)[30], with molecular weights (M+Z = 343.3 and 356.3) indicative of phenazine derivatives (griseolutein A ($C_{17}H_{14}N_2O_6$, $M_w = 342.3$) and D-alanyl-griseolutein ($C_{18}H_{17}N_3O_5$, $M_w = 355.3$), respectively)[31–33].

LysR transcriptional regulator in a fusaric acid resistance operon (*ewf*R-7D5::Tn5). *ewf*R-5D7::Tn5 resulted in loss of antifungal activity *in vitro* (Supplementary Fig. 5a). Tn5 inserted in an operon (*ewf*, Fig. 4h) containing more than five genes required for biosynthesis of the fusaric acid (FA) efflux pump: a predicted *fus*E-MFP/HIYD membrane fusion protein (*ewf*D), *fus*E (*ewf*E) and other membrane proteins (*ewf*B, *ewf*H and *ewf*I)[34,35]. FA (5-butylpyridine-2-carboxylic acid) is a *Fusarium*-encoded mycotoxin antibiotic that interferes with bacterial growth and metabolism[36,37]. Bacterial-encoded FA efflux pumps promote resistance to FA (refs 38,39). Consistent with expectations, *Ewf*R-5D7::Tn5 failed to grow on agar supplemented with FA compared to wild type (Fig. 4i,j). The Tn5 insertion localized to another member of the LysR transcriptional regulator family (*ewf*R), transcribed in the opposite direction as the *ewf* operon. The LysR canonical binding site sequence ($TN_{11}A$)[29] was observed upstream of the *ewf*B–J coding sequences (Fig. 4h). Real-time PCR revealed that *ewf*D/*ewf*E expression was dramatically downregulated in the LysR mutant compared to the wild type (Fig. 4k). Combined, these observations suggest that EwfR is a positive regulator of the *ewf* FA resistance operon and hence suggests that M6 killing activity requires resistance to a toxin (FA) produced by *Fusarium*.

The M6-*ewf* operon is *Fusarium*-inducible. Expression of *ewf*R (LysR regulator of FA resistance) increased threefold after 2 h of exposure to *F. graminearum in vitro* (Fig. 4l). Expression of *ewf*R was also upregulated by FA alone (Fig. 4l). These results demonstrate that M6 can sense *Fusarium* and its diffusible metabolite(s), consistent with our earlier observations (Figs 2 and 3).

Epistatic interaction between phenazine biosynthesis (*ewp*) and FA resistance (*ewf*) operons. FA was previously shown to suppress phenazine biosynthesis by inhibiting quorum sensing

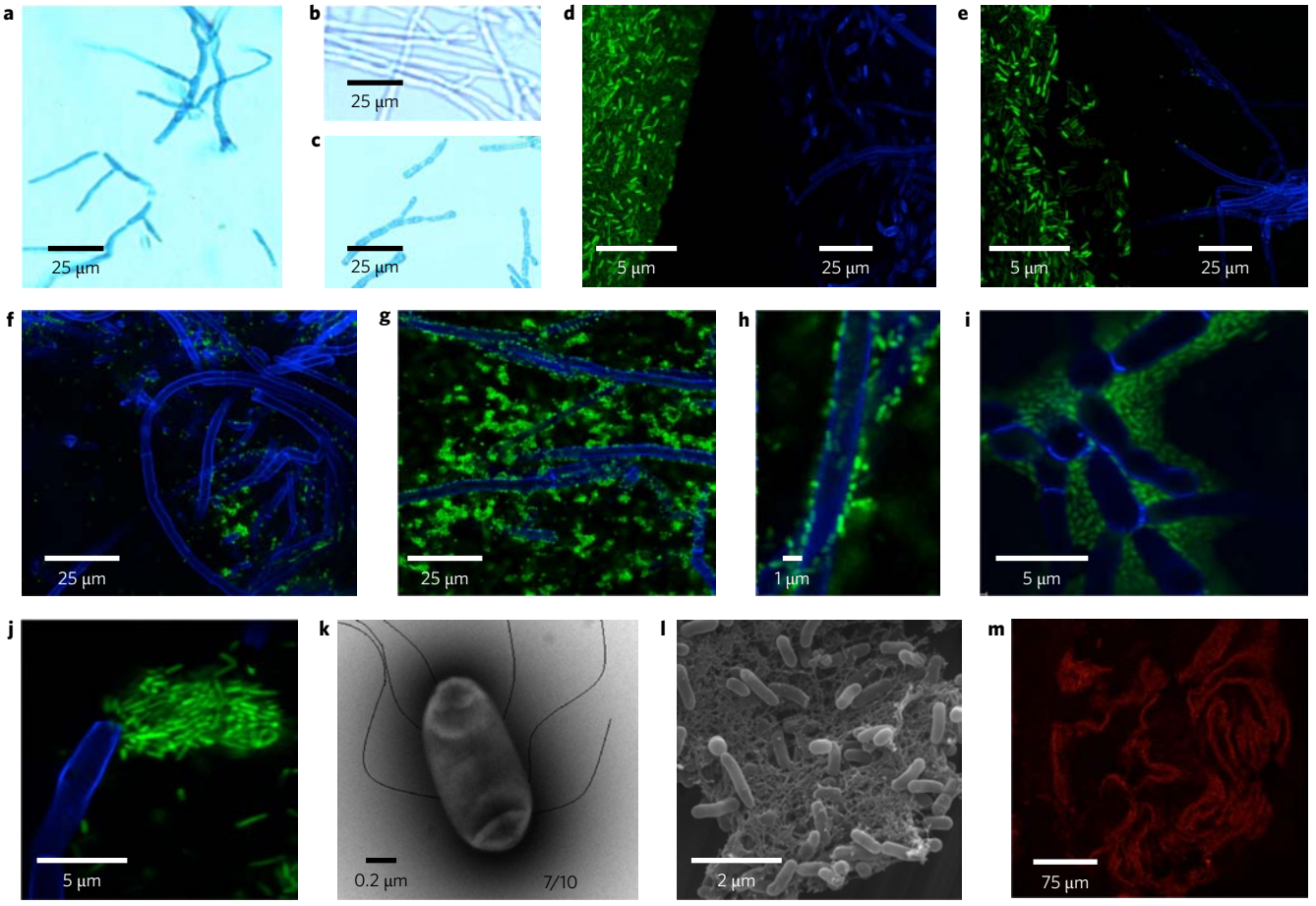

Figure 3 | Behaviour and interactions of endophyte M6 and *F. graminearum in vitro* on microscope slides. a–c, Light microscopy of interactions between *F. graminearum* (Fg) and M6 following staining with Evans blue, which stains dead hyphae blue. Shown are Fg following overnight co-incubation with M6 (**a**), Fg grown away from M6 (control) (**b**) and Fg following overnight co-incubation with a commercial biological control agent (**c**). **d–i**, Time course to illustrate the swarming and attachment behaviour of GFP-tagged M6 (green) to Fg (blue, Calcofluor stained) viewed at 0.5 h (**d**), 1.5 h (**e**), 3 h (**f**), 6 h (**g**), 6 h (**h**, close-up) and 8 h (**i**) following co-incubation. Fg and M6 shown in **d** and **e** were inoculated on the same slide distal from one another at the start of the time course but digitally placed together for these illustrations. **j**, M6 shown breaking Fg hypha. **k**, TEM image of M6 showing its characteristic flagella. The fraction refers to the number of bacteria that were captured that have flagella. **l**,**m**, Biofilm formed by M6 as viewed by SEM (**l**) and confocal microscopy (**m**) in combination with the proteinaceous biofilm stain, Ruby Film Tracer. Pictures are representative of ≥3 biological replicates.

regulatory genes[40]. Interestingly, expression of the putative M6–LysR regulator of phenazine biosynthesis (*ewpR*, see section 'LysR transriptional regulator in a phenazine operon') was downregulated prematurely by FA at log phase (2–3 h), but only when FA resistance was apparently lost (*ewf*R mutant) (Fig. 4m) compared to the wild type (Fig. 4n). The data thus provide evidence for an epistatic relationship between the two LysR genes required for anti-*Fusarium* activity (Fig. 4o). Without this epistatic relationship, a critical M6 antifungal mechanism would be highly impaired by *Fusarium*.

Diguanylate cyclase (*ewg*S-10A8::Tn5). *ewg*S-10A8::Tn5 resulted in loss of antifungal activity *in vitro* (Supplementary Fig. 5a). Tn5 inserted in a gene encoding diguanylate cyclase (EC 2.7.7.65) (*ewg*S) that catalyses conversion of 2-guanosine triphosphate to cyclic dimeric guanosine monophosphate (c-di-GMP), a secondary messenger that mediates quorum sensing and virulence traits[41] (Fig. 5a). Addition of exogenous c-di-GMP restored the antifungal activity of the mutant (Fig. 5b), chemically complementing the mutation. Real-time PCR showed that *ewg*S is not inducible by *Fusarium* (Fig. 5c).

Colicin V production protein (*ewv*C-4B9::Tn5) and *Fusarium* induction. *ewv*C-4B9::Tn5 caused loss of antifungal activity *in vitro* (Supplementary Fig. 5a). Tn5 inserted in a relatively uncharacterized gene required for colicin V production (*ewv*C) orthologous to *cvp*A in *Escherichia coli*[42]. Colicin V is a secreted peptide antibiotic[43]. Consistent with the gene annotation, *ewv*C-4B9::Tn5 failed to inhibit an *E. coli* strain that is sensitive to colicin V compared to wild type (Fig. 5d). Real-time PCR showed that *ewv*C expression increased sixfold after co-incubation with *F. graminearum* at log phase (Fig. 5e), providing additional evidence that M6 can sense *Fusarium*.

Effect of mutants on other virulence traits. As motility, attachment and biofilm formation by M6 were critical for its anti-*Fusarium* activity *in planta* (Fig. 2) and *in vitro* (Fig. 3), the M6–Tn5 mutants were analysed for these virulence traits *in vitro* (Fig. 6, Supplementary Table 5 and Supplementary Fig. 6). Compared to wild-type M6, the two *Lys*R regulatory mutants (*ewp*R, *ewf*R) showed significant reductions in motility (Fig. 6b,c), swarming (Fig. 6g,h) and associated flagella formation (Fig. 6l,m), loss of attachment to *Fusarium* hyphae (Fig. 6q,r) and loss of biofilm (Fig. 6v,w and Supplementary Fig. 6b,c,f). These results suggest that the LysR proteins regulate virulence genes in addition to phenazine biosynthesis and FA resistance. The *ewg*S mutant, disrupted in the formation of the secondary messenger c-di-GMP,

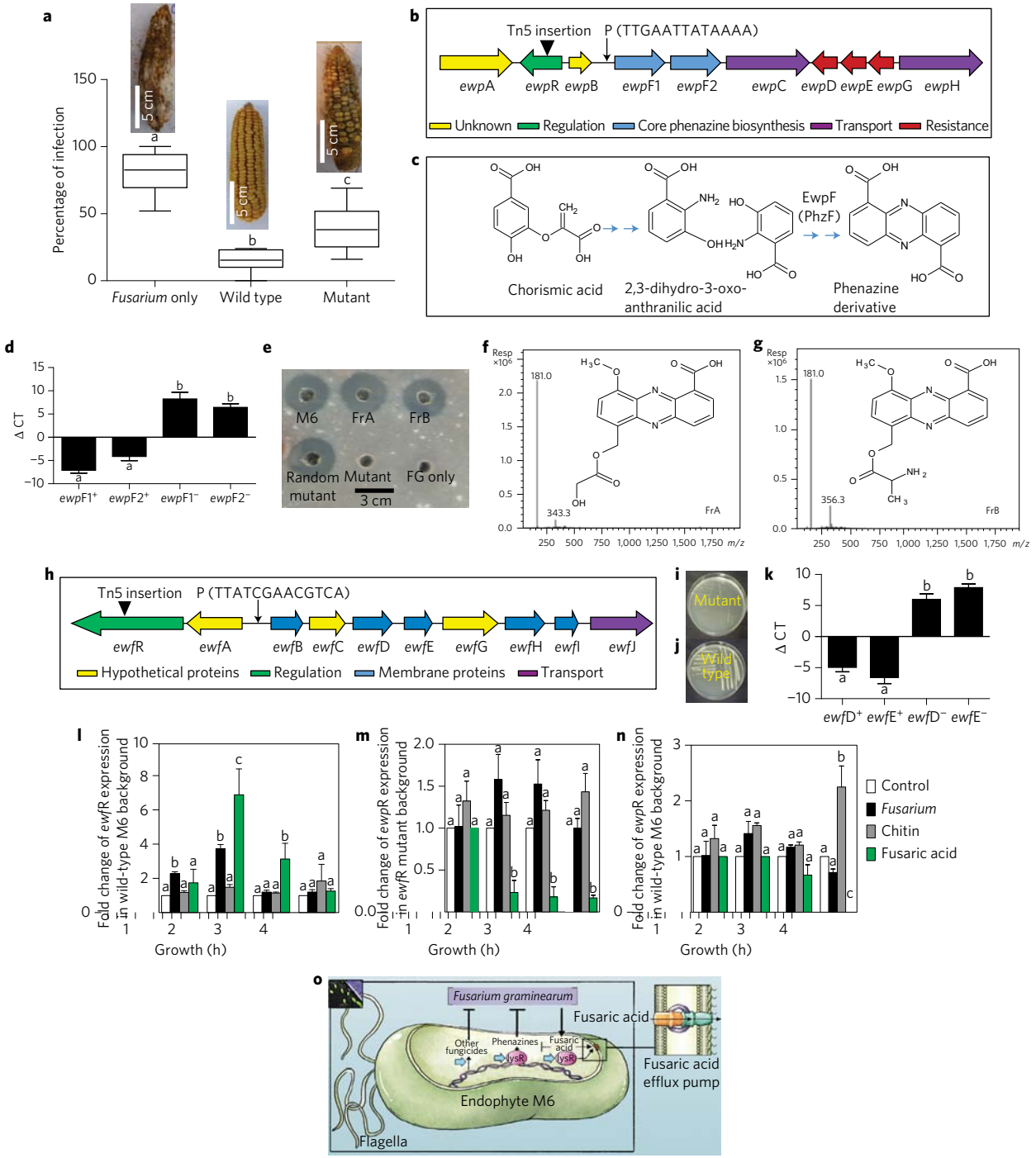

Figure 4 | Characterization of phenazine mutant *ewp*R-5D7::Tn5 and FA resistance mutant *ewf*R-7D5::Tn5 and their interactions. a–g, Characterization of phenazine mutant *ewp*R-5D7::Tn5: effect of M6 mutant *ewp*R$^-$ on suppression of *F. graminearum* (Fg) in maize compared to wild-type M6 and Fg-only, with representative maize ear pictures (**a**); genomic organization of the predicted phenazine biosynthetic operon showing the Tn5 insertion site and putative LysR binding site within the promoter (P) (**b**); phenazine biosynthetic pathway (**c**); quantitative real-time PCR (qRT-PCR) of the two core phenazine genes (*ewp*F1, *ewp*F2) in wild-type M6 (+) and mutant (–) (*ewp*R$^-$) (**d**); agar diffusion assay showing the inhibition of Fg growth by methanol extracts of wild-type M6, two wild-type fractions (FrA, FrB), *ewp*R$^-$ mutant (mutant), a random Tn5 insertion or buffer (**e**); mass spectroscopy of putative phenazine derivatives in wild-type M6 fractions A and B (**f**,**g**). **h–k**, Characterization of FA resistance mutant *ewf*R-7D5::Tn5: genomic organization of the predicted FA resistance operon showing the Tn5 insertion site and putative LysR binding site within the promoter (P) (**h**); inhibitory effect of FA on the growth of mutant *ewf*R$^-$ compared to wild-type M6 (**i**,**j**); qRT-PCR of two genes required for formation of the FA efflux pump (*ewf*D, *ewf*E) in wild-type M6 (+) and mutant *ewf*R$^-$ (–) (**k**). **l–n**, qRT-PCR of wild-type *ewf*R expression in a wild-type M6 background (**l**), wild-type *ewp*R in an *ewf*R$^-$ mutant background (**m**), and wild-type *ewp*R in a wild-type M6 background (**n**). **o**, Summary of the interactions between M6-derived phenazine, *Fusarium*-derived FA and M6-derived FA resistance (efflux pump). Cartoon is courtesy of L. Smith (University of Guelph) for re-use under the Creative Commons BY licence. Whiskers in **a** represent the range of data points. Error bars in **d** and **k–n** indicate the standard error of the mean. For greenhouse disease trials (**a**), $n = 10$ biological replicates. For other experiments, $n = 3$ biological replicates. For graphs shown in **a**, **d**, **k** and **l–n**, letters that are different from one another indicate means that are statistically different (within a time point for **l–n**) using Mann–Whitney *t*-tests ($P \leq 0.05$). Pictures are representative of 10 biological replicates (**a**) or ≥3 biological replicates (**e**,**i**,**j**).

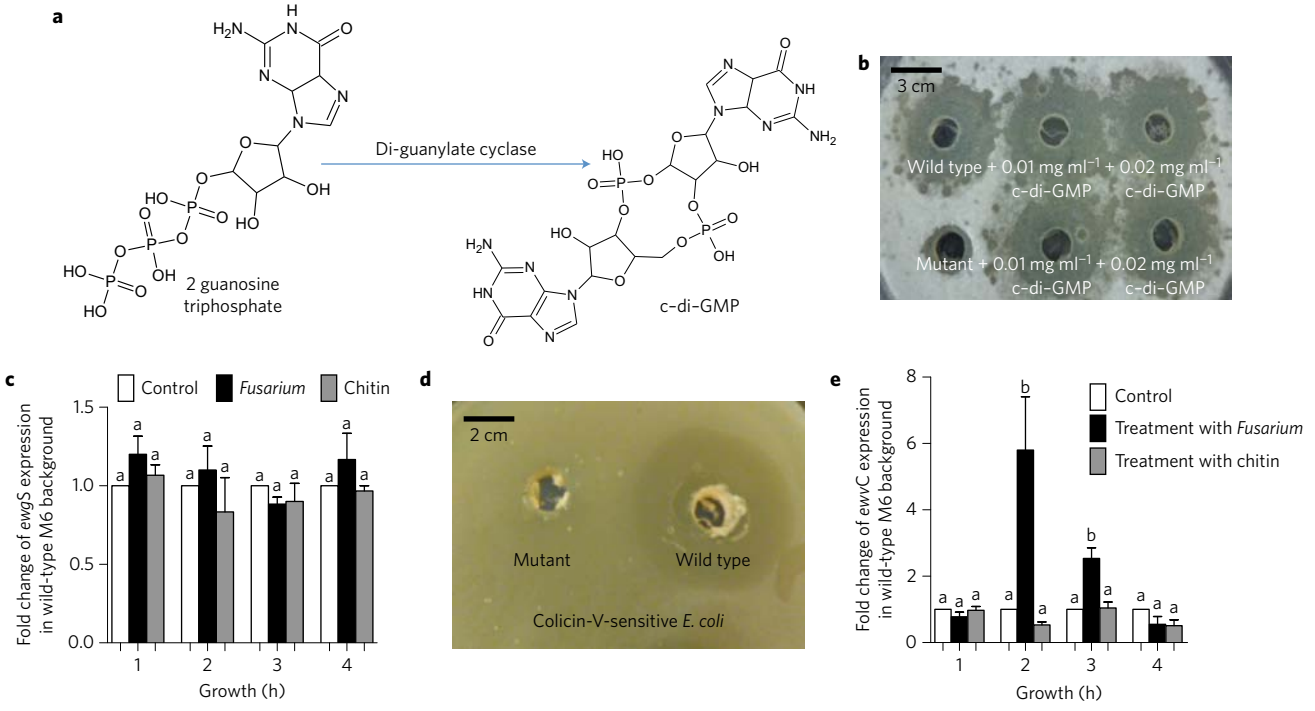

Figure 5 | Characterization of di-guanylate cyclase mutant *ewg*S-10A8::Tn5 and colicin V mutant *ewv*C-4B9::Tn5. a–c, Characterization of mutant *ewgS*-10A8::Tn5: illustration of the enzymatic conversion of 2 guanosine triphosphate to c-di-GMP catalysed by di-guanylate cyclase (**a**); complementation of the putative *ewgS*$^{-}$ mutant with respect to inhibition of *F. graminearum* (Fg) by addition of c-di-GMP (0.01 and 0.02 mg ml^{-1}), compared to wild-type strain M6 (**b**); qRT-PCR analysis of wild-type *ewg*S expression in a wild-type M6 background (**c**). **d**,**e**, Characterization of mutant *ewv*C-4B9::Tn5: dual culture agar diffusion assay showing loss of antagonism against the colicin V sensitive *E. coli* strain (MC4100) by the *ewv*C^{-} mutant compared to wild-type M6 (**d**); qRT-PCR analysis of wild-type *ewv*C expression in a wild-type M6 background (**e**). Error bars in **c** and **e** indicate standard error of the mean. For all experiments, $n = 3$ biological replicates. For graphs shown in **c** and **e**, letters that are different from one another indicate that their means are statistically different ($P \leq 0.05$) using Mann–Whitney *t*-tests ($P \leq 0.05$). Pictures are representative of ≥3 biological replicates (**b**,**d**).

generally showed more severe loss-of-function phenotypes (Fig. 6d, i,n,s,x; Supplementary Fig. 6d,f), consistent with its predicted upstream role in regulating virulence traits. The *ewv*C mutant, disrupted in colicin V antibiotic production, showed only limited reductions in motility, swarming and flagella formation (Fig. 6e,j, o) and maintained the ability to attach onto *Fusarium* hyphae and produce biofilm (Fig. 6t,y; Supplementary Fig. 6e,f).

Discussion

RHESt is a novel plant defence mechanism. Here, we have reported that an endophyte (M6) from the ancient African cereal, finger millet, swarms towards invading *Fusarium* hyphae, attracted by a yet unknown mechanism derived from *Fusarium* itself or the host plant responding to *Fusarium*. M6 then builds a remarkable physicochemical barrier, resulting from RHESt at the rhizosphere–root interface (rhizoplane) that prevents entry and/or traps *Fusarium* for subsequent killing. These results show that an endophyte can create its own specialized killing microhabitat. M6 provides further support for our hypothesis[44] that plants have retained some endophytes because they are mobile hunters of host pathogens, analogous to immunity cells in animals, to protect plant cells, which are immobile. Indeed, RHESt is an inducible structure that only forms in the presence of *Fusarium*.

RHESt consists of multiple lines of defence, a dense layer of stacked, elongated root hairs intercalated with endophyte micro-colonies, followed by a continuous endophyte barrier layer on the rhizoplane (for a summary model see Supplementary Fig. 7). M6 is associated with induced growth of the root hairs, which then bend to form the RHESt scaffold, probably mediated by biofilm formation and attachment. *In vitro*, M6 synthesizes auxin (indole acetic acid (IAA)) (Supplementary Fig. 4), a hormone known to stimulate root hair growth[45]. Root hair bending associated with RHESt might be an active process, similar to rhizobia-mediated root hair curling[46], or an indirect consequence of microcolony attachment to adjacent root hairs. RHESt represents a plant defence strategy not previously captured, to the best of our knowledge.

M6-mediated killing requires genes that encode the following: signal-amplifying regulatory factors (LysR, c-di-GMP); resistance to a *Fusarium*-derived antibiotic (FA, see section 'M6–*Fusarium*–millet co-evolution'); and antimicrobial agents including phenazine(s), colicin V and additional candidates such as chitinase (Supplementary Fig. 8a), phenylacetic acid and P-amino-phenyl-alanine (Supplementary Table 5). Mutant phenotypes suggest that the two LysR regulators, and especially c-di-GMP, also regulate other virulence traits including motility, biofilm formation and attachment to *Fusarium*.

M6–*Fusarium*–millet co-evolution. We have previously demonstrated that finger millet also hosts fungal endophytes that secrete anti-*F. graminearum* metabolites[4]. These observations, combined with mutants from this study that demonstrate that no single antifungal mechanism is sufficient for M6 to combat *Fusarium*, suggest that the millet endophyte community has been engaged in a step-by-step arms race with *Fusarium*, resulting in the endophytes having a diverse arsenal, some of which presumably act within RHESt (Fig. 2i,j). Consistent with this interpretation, the antifungal activity of M6 requires resistance to the *Fusarium*-derived antibiotic FA, which would otherwise inhibit biosynthesis of the M6-derived fungicide phenazine. Our results further show a novel epistatic regulatory interaction between M6-encoded FA resistance and phenazine biosynthesis, wherein an M6-encoded LysR activator of FA resistance prevents FA from suppressing the M6-encoded LysR regulator of

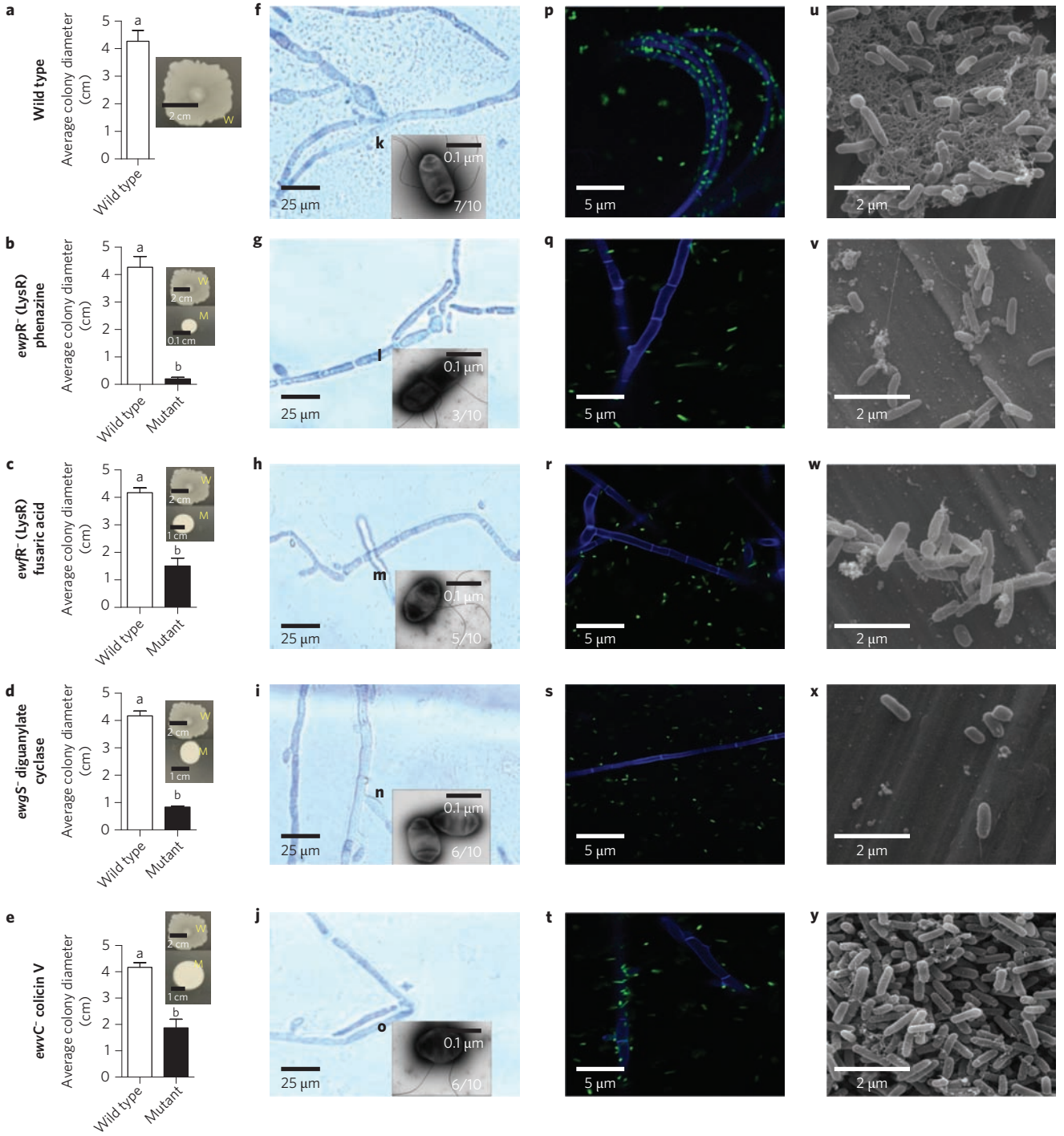

Figure 6 | Microscopy imaging of other virulence traits associated with wild-type M6 (W) and each mutant (M). a–e, Quantification of motility and a representative image (inset) of the motility assays on a semisolid agar plate of wild-type M6 (**a**) compared to each mutant (**b–e**). **f–j**, Light microscopy image showing swarming and colony formation around *F. graminearum* (stained with lactophenol blue) by wild-type M6 (**f**) compared to the mutants (**g–j**). **k–o**, TEM images showing the strain phenotype and number of flagella in wild-type M6 (**k**) compared to the mutants (**l–o**). Numbers indicate the fraction of biological replicates that share the phenotype shown. **p–t**, Confocal microscopy images showing the attachment of wild-type M6 (**p**) or the mutants (**q–t**) (green) to *F. graminearum* hyphae (stained blue with Calcofluor). **u–y**, SEM images to visualize biofilms associated with wild-type M6 (**u**) compared to the mutants (**v–y**). Error bars in **a–e** indicate standard error of the mean. For all experiments, $n = 3$ biological replicates. For all graphs, letters that are different from one another indicate that their means are statistically different using Mann–Whitney *t*-tests ($P \leq 0.05$). Pictures are representative of ≥3 biological replicates. See Supplementary Table 5 for additional data.

phenazine biosynthesis (Fig. 4m,n). FA was previously shown to interfere with the biosynthesis of phenazine via a quorum sensing-mediated pathway[40]. We propose that the phenazine–FA arms race provides evidence that M6 and *Fusarium* co-evolved. This co-evolution may have been tripartite, involving the millet genome, given the involvement of root hairs in RHEST and the observation that M6 secretes 2,3-butanediol (genome mining and Supplementary Fig. 8b), a hormone known to elicit plant defences[47].

Interactions and real-world implications. This study suggests that M6 probably benefits subsistence millet farmers, not only by suppressing *Fusarium* in plant tissues, but also in seeds after harvest. Under poor seed drying and storage conditions that mimic those of subsistence farmers, M6 caused dramatic reductions in DON (Fig. 1m,r), a potent human and livestock mycotoxin. Thus, for thousands of years, subsistence farmers may have inadvertently selected for the physicochemical RHESt barrier ability of M6, by selecting healthy plants and their seeds. M6 inhibited the growth of five other fungi including two additional *Fusarium* species (Supplementary Table 2), suggesting that RHESt may contribute to the broad-spectrum pathogen resistance of millet reported by subsistence farmers. Under controlled conditions, the benefits of M6 were transferable to maize and wheat (Fig. 1i,o), which are severely afflicted by *F. graminearum* and DON. Field testing will determine the efficacy of M6 under real-world conditions that include soil-derived microbial competitors. Further studies are needed to determine whether the anti-*F. graminearum* fungal endophytes of millet[4] cooperate with M6 in RHESt or act at other susceptible locations, and how M6 functions in heterologous hosts and tissues. For example, our group has shown different endophytes within a community interact with one another to stimulate biosynthesis of a fungicide[48].

Finger millet is a scientifically neglected crop that grows under a variety of stresses including native pathogens such as *Fusarium*[1,2]. This study and earlier results[44] suggest that endophytes that show non-distinct localization under optimal conditions should be retested under native stress conditions. The discovery of RHESt suggests that other scientifically neglected, ancient crops may be worth exploring for microbiome–host interactions.

Methods

Isolation, identification and antifungal activity of endophytes. Commercial finger millet seeds originating from Northern India were grown on clay Turface in the summer of 2012 according to a previously described method[4]. Tissue pool sets (three sets of 5 seeds, 5 shoots and 5 root systems from pre-flowering plants) were surface-sterilized following a standard protocol[4]. Surface-sterilized tissues were ground in lysogeny broth (LB) liquid medium in a sterilized mortar and pestle, then 50 µl suspensions were plated onto two types of agar plates (LB and Biolog Universal Growth). Plates were incubated at 25, 30 and 37 °C for 1–3 days. A total of seven bacterial colonies (M1–M7) were purified by repeated culturing on fresh media. For molecular identification of the isolated bacterial endophytes, PCR primers (Supplementary Table 7) were used to amplify and sequence 16S rDNA as previously described[7], followed by best BLAST matching to GenBank. 16S rDNA sequences have been deposited in GenBank (KU307449–KU307455). Phylogenetic trees of finger millet endophytes were generated using Phylogeny.fr software[49,50]. SEM imaging was used to phenotype the candidate bacterium, as previously described[7], using a Hitachi S-570 microscope (Hitachi High Technologies) at the Imaging Facility, Department of Food Science, University of Guelph.

To test the antifungal activity of the isolated endophytes against *F. graminearum*, agar diffusion dual culture assays were undertaken ($n = 3$ biological replicates). Nystatin (catalogue no. N6261, Sigma Aldrich) and amphotericin B (catalogue no. A2942, Sigma Aldrich) were used as positive controls at 10 and 5 µg ml^{-1}, respectively, while the negative control was LB medium. Using a similar methodology, additional antifungal screening was conducted using the Fungal Type Culture Collection at Agriculture and Agrifood Canada (Supplementary Table 2).

Microscopy imaging

In planta *colonization of the candidate antifungal endophyte M6.* To verify the endophytic behaviour of the candidate antifungal bacterium M6 in maize, wheat and millet, the bacterium was subjected to tagging with green fluorescent protein (GFP) (vector pDSK-GFPuv)[51] and *in planta* visualization using confocal scanning microscopy at the Molecular and Cellular Imaging Facility, University of Guelph, Canada.

In vitro *interaction using light microscopy.* Both the fungus and bacterium M6 were allowed to grow in close proximity to each other overnight on microscope slides coated with a thin layer of potato dextrose agar (PDA). Thereafter, the fungus was stained with the vitality stain Evans blue, which stains dead hyphae blue. The positive control was a commercial biological control agent (*B. subtilis* QST*713*, Bayer CropScience, batch no. 00129001) (100 mg/10 ml). Pictures were captured using a light microscope (BX51, Olympus).

In vitro *and* in planta *interactions using confocal microscopy.* All the experiments were conducted using a Leica TCS SP5 confocal laser scanning microscope at the Molecular and Cellular Imaging Facility at the University of Guelph, Canada.

To visualize the interactions between endophyte M6 and *F. graminearum* inside finger millet, finger millet seeds were surface sterilized and coated with GFP-tagged endophyte and then planted on sterile based medium in glass tubes, each with four to five seeds. Phytagel medium was prepared as previously described[4]. At 14 days after planting, finger millet seedlings were inoculated with *F. graminearum* (50 µl of a 48 h old culture grown in potato dextrose broth) and incubated at room temperature for 24 h. The control consisted of seedlings incubated with potato dextrose broth only. There were three tubes (biological replicates) for each treatment. Thereafter, roots were stained with Calcofluor florescent stain (catalogue no. 18909, Sigma-Aldrich), which stains chitin blue, following the manufacturer's protocol, then scanned.

To visualize the attachment of bacterium M6 to fungal hyphae, GFP-tagged M6 and *F. graminearum* were inoculated overnight at 30 °C on microscope slides covered with a thin layer of PDA. Thereafter, the fungal hyphae were stained with Calcofluor and examined. The same protocol was used to test if this recognition was disrupted in the Tn5 mutants.

Experimental set-up for the three-dimensional RHESt image and video. To precisely control the location of *F. graminearum* infection, a modified set-up was used. Finger millet seeds were surface-sterilized and coated with GFP-tagged endophyte (as above) and then planted on sterile Phytagel-based medium in 150-mm-diameter Petri dishes, each with two seeds. Phytagel medium was prepared as previously described[4], except a higher concentration of Phytagel was used (4 g l^{-1}). The plates were placed vertically in a plant growth cabinet (22 °C, 16 h light/8 h dark, with 80–100 µmol m^{-2} s^{-1} cool white fluorescent light). At 12 days after planting, dishes were spot-inoculated with *F. graminearum* (10 µl of a 48 h old culture grown in potato dextrose broth) onto the gel surface on one side of the root (at a distance of 0.5 cm, spread parallel to the rhizoplane starting 1 cm from the root tip using a sterile cotton swab) and incubated for 72 h in the same growth cabinet under the same conditions. Subsequently, roots were stained with Calcofluor florescent stain (catalogue no. 18909, Sigma-Aldrich) following the manufacturer's protocol, and then placed onto microscope slides mounted in 100% glycerol and scanned. A deep confocal stack (90 µm thickness) was recorded and rendered as a three-dimensional video.

Biofilm imaging. To test the ability of endophyte M6 or each of the mutants to form a biofilm, SEM imaging was conducted. Each genotype was inoculated into 200 µl LB medium in a 96-well plate. Each well had a 304H food-grade stainless-steel coupon to allow for bacterial adherence (designed at the Physical Workshop, Department of Physics, University of Guelph). The plate was incubated at 37 °C and 50 r.p.m. To remove planktonic cells, the biofilms were washed with 1× PBS for 10 min after 24 h of inoculation, then reinserted into fresh LB medium. The process was repeated every 24 h for 5 days, under sterile conditions. The biofilms were then fixed on the stainless-steel coupons with glutaraldehyde and prepared for SEM following a standard procedure (Electron Microscopy Facility, McMaster Children's Hospital). Non-inoculated LB medium was used as a control. The entire experiment was repeated in duplicate.

To confirm the result obtained by SEM, confocal imaging was conducted. Each genotype was inoculated into 40 ml LB, in a Falcon tube containing a sterile microscope glass slide to allow for bacterial adhesion. The biofilms were allowed to develop as described above. The biofilm matrix on each slide was detected using FilmTracer SYPRO Ruby Biofilm Matrix Stain (F10318, ThermoFisher Scientific) using the manufacturer's protocol and then examined using a Leica TCS SP5 confocal laser scanning microscope (Molecular and Cellular Imaging Facility, University of Guelph). The entire experiment was repeated three times.

Testing the ability of M6 to produce IAA. Endophytic IAA (auxin) production was measured as previously described[52]. Strain M6 was cultured on LB agar plates supplemented with 5 mM L-tryptophan, then incubated at 30 °C for 3 days, with three biological replicates. A nitrocellulose membrane was placed on M6 colonies and the plates were incubated at 4 °C for 24 h. Whatman # 2 filter papers were placed into fresh Petri dishes, saturated with Salkowski reagent (0.01 M ferric chloride in 35% perchloric acid), and the nitrocellulose membranes were shifted onto the filter paper. A change in colour to pink or red surrounding the colonies indicated IAA production. Results were compared to a positive control (bacterial endophyte strain E10)[53].

Suppression of *F. graminearum* and DON accumulation in storage in wheat. The candidate anti-*Fusarium* endophyte M6 was tested for its ability to suppress *F. graminearum* in Quantum spring wheat (C&M Seeds) in biologically replicated greenhouse trials (Crop Science Greenhouse Facility, University of Guelph).

Seed treatment. Seeds of spring wheat were surface -sterilized as follows: seeds were washed in 0.1% Triton X-100 detergent with shaking for 10 min; the detergent was

poured off, 3% sodium hypochlorite was then added (twice for 10 min), which was followed by rinsing with distilled, autoclaved water, washing with 95% ethanol for 10 min and finally the seeds were washed five to six times with distilled, autoclaved water. Complete surface sterilization was verified by inoculating the last wash on LB plates at 37 °C; none of these washes showed growth. The seeds were then coated with the endophyte. To prepare endophyte inoculant, M6 was incubated at 37 °C for 24 h in LB medium, centrifuged, washed and re-suspended in PBS buffer to an optical density at 600 nm (OD_{600}) of 0.5. Afterwards, 500 µl of M6 was rocked for 2 h on a horizontal shaker (Serial #980216M, National Labnet Company) with 10 ml polyvinyl pyrrolidine (PVP, catalogue no. 9003398, Sigma Aldrich), which was used as a seed-coating agent. Endophyte- or buffer-coated seeds were germinated on wet paper towels in the dark for 7 days. Uniformly sized seedlings were then moved to pots containing Turface clay (Turface Athletics) in a greenhouse.

Pathogen treatment. Pathogen spores were prepared as follows. The liquid spore suspension medium was prepared using distilled water as follows (per l): 2 g KNO_3, 2 g KH_2PO_4, 1 g $MgSO_4$, 1 g KCl, 1 g dextrose, 20 mg/100 ml (each) of minor elements ($FeCl_2$, $ZnSO_4$, $MnSO_4$). Subsequently, 350 ml of the medium was added to 2 l flasks, then sterilized at 121 °C for 10 min. Followed by cooling at room temperature, three to four PDA plugs of *F. graminearum* or 10 ml liquid conidia suspensions were added to each flask under sterile conditions and these were subsequently incubated on shaker tables under a 12:12 h ultraviolet light: dark cycle for approximately two weeks at room temperature. Each spore solution was standardized to 20,000 spores per ml with a haemocytometer, then refrigerated or used to treat plants directly. Per plant, 1 ml of the *F. graminearum* spore suspension (20,000 spores per ml) was then sprayed directly onto wheat heads at the flowering stage with the emergence of anthers (flowers in anthesis, as anthers are the primary sites of infection). No surfactant or other formulation agents were used.

Endophyte treatment. The bacterium M6 was introduced twice more to ensure its high titre: the first endophyte spray was performed simultaneously with the pathogen (at the flowering stage with the emergence of anthers), while the second spray was the endophyte alone, 3 days later. M6 was grown overnight in LB medium then 1 ml of OD_{600} 0.4–0.6 was used for spraying. No surfactant or other formulation agents were used.

Control treatments. For the positive control, seeds were coated with PVP followed by fungicide spraying (PROLINE 480 SC Foliar Fungicide, Bayer Crop Science), at a concentration of 200 g active ingredient per hectare, on mature wheat heads before infection with the fungal pathogen; no endophytes were introduced. The negative control consisted of seeds coated with PVP followed by repeated spraying with 1 ml LB medium (as buffer control), along with the pathogen inoculation (as described above).

Experimental design and growth conditions. Each treatment group consisted of 20 plants arranged in a randomized block design. Two independent greenhouse trials were conducted in the summer of 2013. The growth conditions were as follows: 28 °C/20 °C, 16 h:8 h, ≥800 µmol m^{-2} s^{-1} at pot level, with metal halide and high-pressure sodium lamps supplemented with GroLux lighting, fertilized using drip irrigation containing modified Hoagland's solution, until seed maturity[54]. During the *Fusarium* or endophyte spray treatments, the greenhouse temperature was 28–30 °C. To promote *Fusarium* growth, the greenhouse was sprayed twice per week with water to achieve a typical relative humidity of ~60–80%.

Post-maturation conditions. Following grain head maturation, watering was ceased and plants were allowed to dry for an average of 18 days in the greenhouse under the same conditions as the growth phase (28 °C/20 °C, 16 h:8 h) but without added humidity (all spraying was ceased). Grains were then threshed, and then stored in sealed paper envelopes for 14 months under ambient conditions in a laboratory (temperature ~18–25 °C, moisture content of ~40–60%).

Disease scoring. At full maturity, following seed drying, disease was scored as the percentage of grains per plant with visually observable disease symptoms relative to the total number of grains per plant. The infected seeds were defined as having a rough, shrivelled surface and/or white hyphae[55]. Total dry grain weight at harvest per plant was also measured. Results were analysed and compared using Mann–Whitney *t*-tests ($P \leq 0.05$). Prism Software v5 (GraphPad Software) was used for the statistical analysis.

DON mycotoxin analysis. Enzyme-linked immunosorbent assay (ELISA) analysis was conducted to test the accumulation of DON in seeds after 14 months of storage in conditions that mimic those of African subsistence farmers (temperature ~18–25 °C, moisture content of ~40–60%).

Suppression of *F. graminearum* and DON accumulation in storage in maize. Bacterium M6 was tested *in planta* for its ability to suppress *F. graminearum* in maize (hybrid P35F40, Pioneer HiBred) in two independent greenhouse trials as previously described[7]. As in wheat, ELISA analysis was conducted to test the accumulation of DON in seeds after 14 months of storage in conditions that mimic those of African subsistence farmers (temperature ~18–25 °C, moisture content of ~40–60%). Control treatments consisted of plants subjected to pathogen inoculation only and plants subjected to pathogen inoculation followed by prothioconazole fungicide spraying (PROLINE 480 SC, Bayer Crop Science). Results were analysed and compared using Mann–Whitney *t*-tests ($P \leq 0.05$).

Transposon mutagenesis, gene rescues and complementation. To identify the genes responsible for the antifungal activity, Tn5 transposon mutagenesis was conducted using the EZ-Tn5<R6Kγori/KAN-2>Tnp Transposome kit (catalogue no. TSM08KR, Epicentre) according to the manufacturer's protocol. Genomic DNA of the candidate Tn5 mutants was extracted using a Bacterial Genomic DNA Isolation Kit (#17900, Norgen Biotek). One microgram of the extracted DNA was digested with *Bam*HI (#15201023, Invitrogen) at 37 °C for 1 h, then purified using Illustra GFX PCR DNA and Gel Band Purification Kits. The purified DNA fragments were allowed to self-ligate for 1 h at room temperature using ExpressLink T4 DNA Ligase (A13726, Invitrogen) then purified using Illustra GFX PCR DNA and Gel Band Purification Kits. Two microlitres of each ligation mixture were used to transform TransforMax EC100D pir-116 electrocompetent *E. coli* (EC6P095H, Epicentre) by electroporation (as described above). Plasmid DNA was extracted from recovered colonies using a QIAprep Spin Miniprep Kit (#27106, Qiagen). To identify the open reading frame of each disrupted gene, Tn5 transposon- specific read out primers, KAN-2 FP-1 forward primer with sequence 5′-ACCTACAACAAAGCTCTCATCAACC-3′ and R6KAN-2 RP-1 reverse primer with sequence 5′-CTACCCTGTGGAACACCTACATCT-3′ were used for sequencing at the Genomics Facility, University of Guelph.

The mutants were screened for loss of anti-*Fusarium* activity using the agar dual culture method compared to wild type. Insertion mutants that completely lost the antifungal activity *in vitro* were further tested for loss of *in planta* activity using maize as a model in two independent greenhouse trials (same protocol as above, Suppression of *F. graminearum* and DON accumulation in storage in maize). The sequences flanking each candidate Tn5 insertion mutant of interest were identified using plasmid rescues according to the manufacturer's protocol. The rescued gene sequences were BLAST searched against the whole genome sequence of bacterium M6 (ref. 24). Operons were tentatively predicted using FGENESB (ref. 56) from Softberry. Promoter regions were predicted using PePPER software (University of Groningen)[57]. To confirm the identity of the gene as discovered by Tn5 mutagenesis, each mutant was complemented with the corresponding predicted wild-type coding sequence, which was synthesized (VectorBuilder, Cyagen Biosciences) using a pPR322 vector backbone (Novagen) under the control of the T7 promoter. Two microlitres of each synthesized vector was electroporated using 40 µl electrocompetent cells of the corresponding mutant. The transformed bacterium cells were screened for gain of the antifungal activity against *F. graminearum* using the dual culture assay as described above.

Quantitative real-time PCR to measure gene expression of the candidate antifungal genes. To test if the candidate genes are inducible by *F. graminearum* or constitutively expressed, real-time PCR analysis was conducted using gene-specific primers designed using Primer Express software 3.0 (Supplementary Table 7). Wild-type strain M6 or mutant strain was grown overnight in LB medium (37 °C, 225 r.p.m.). Thereafter, the culture was transferred to fresh sterilized LB medium (1:100) to a final OD_{600} of 0.02 then allowed to grow (37 °C, 225 r.p.m.) until OD_{600} = 0.14. The culture was divided under sterile conditions into three or four flasks, 100 ml each. To one flask, 3 ml of 48 h old *F. graminearum* grown in potato dextrose broth was added. To the second flask, 0.1 g pre-sterilized chitin (catalogue no. C7170, Sigma Aldrich) and 3 ml potato dextrose broth were added. To the third flask, the blank control, only 3 ml potato dextrose broth was added (blank control). To the fourth flask, sub-inhibitory concentration of FA (0.005) was added. The flasks were incubated under the same conditions (37 °C, 250 r.p.m.). Following incubation, 1 ml samples were collected from each flask at regular time intervals (1 h (OD_{595} = 0.3), 2 h (OD_{595} = 1.1), 3 h (OD_{595} = 1.4) and 4 h (OD_{595} = 1.4–1.5)) until the bacterial growth reached the stationary phase. RNA was extracted following a standard protocol (E.Z.N.A Total RNA kit, catalogue no. R6834–01, Omega Bio-tek). To remove any DNA contamination from the extracted RNA, samples were treated with a DNA-free Kit (AM1906, Ambion) following the manufacturer's protocol. RNA samples were analysed by qPCR at the Genomics Facility, University of Guelph. RNA quality was checked using Bioanalser 2100 (Agilent). cDNA was made using a cDNA Reverse Transcription Kit (#4368814, Applied BioSystems). The 20 µl reaction mixture for real-time PCR consisted of 1 µl MultiScribe Reverse Transcriptase (50 U $µl^{-1}$), 2 µl 10× reverse transcription buffer, 2 µl 10× random primers, 0.8 µl 25× (100 mM) dNTPs, 10 µl RNA (90 ng $µl^{-1}$) and 4.2 µl nuclease-free water. The reverse transcription conditions were 10 min at 25 °C, 120 min at 37 °C, 5 min at 85 °C, hold at 4 °C. After completion of this cycle, 120 µl water was added to 20 µl cDNA, then 5 µl was used in each qPCR reaction. Each qPCR reaction mixture consisted of 5 µl cDNA, 10 µl 2× PerfeCTa SYBR Green FastMix with ROX (Quanta BioScience), 0.8 µl forward and reverse primer (5 µM) and 4.2 µl nuclease-free water. 16S primers were used as a housekeeping gene to normalize the gene expression data. For the housekeeping gene, a 400× dilution primer was used. The conditions for qPCR were 30 s at 95 °C and 40 cycles of 3 s at

95 °C and 30 s at 60 °C. Gene expression was calculated using Delta Ct (cycle threshold), where Delta Ct = Ct gene of interest − Ct housekeeping gene.

Mutant phenotyping

Transmission electron microscopy (TEM). To phenotype the candidate mutants, TEM imaging was conducted. Wild-type strain M6 and each of the candidate mutants were cultured overnight in LB medium (37 °C, 250 r.p.m.). Thereafter, 5 µl of each culture was pipetted onto a 200-mesh copper grid coated with carbon. The excess fluid was removed onto a filter, and the grid was stained with 2% uranyl acetate for 10 s. Images were taken by a F20 G2 FEI Tecnai microscope operating at 200 kV equipped with a Gatan 4 K charge-coupled device camera and Digital Micrograph software at the Electron Microscopy Unit, University of Guelph.

Motility assay. Wild-type or mutant strains were cultured overnight in LB medium (37 °C, 225 r.p.m.). The OD_{595} for each culture was adjusted to 1.0, then 15 µl of each culture was spotted onto the centre of a semisolid LB plate (0.3% agar) and incubated overnight (37 °C, no shaking). Motility was measured as the diameter of the resulting colony. There were ten biological replicates for each culture. The entire experiment was repeated independently.

Swarming test. To examine the ability of the strains to swarm and form colonies around the fungal pathogen, *in vitro* interaction/light microscopy imaging was conducted. Wild-type M6 and each mutant were incubated with *F. graminearum* on microscope slides coated with PDA. *F. graminearum* hyphae was stained with lactophenol blue solution (catalogue no. 61335, Sigma-Aldrich) then examined under a light microscope (B1372, Axiophot, Zeiss) using Northern Eclipse software.

Biofilm spectroscopic assay. For further details see section 'Biofilm imaging'. To test the ability of the strains to form biofilms, all putative mutant strains were initially cultured overnight in LB medium (37 °C and 250 r.p.m.), and adjusted to an OD_{600} of 0.5. Cultures were diluted in LB (1:100), then 200 µl from each culture was transferred to a 96-well microtitre plate (3370, Corning Life Sciences) in six biological replicates. The negative control was LB medium only. The microtitre plate was incubated for 2 days at 37 °C. The plate was emptied by aspiration and washed three times with sterile saline solution. Adherent cells were fixed with 200 µl 99% methanol for 15 min then air-dried. Thereafter, 200 µl 2% crystal violet (94448, Sigma) was added to each well for 5 min then washed with water, and left to air dry. Finally, 160 µl 33% (vol/vol) glacial acetic acid was added to each well to solubilize the crystal violet stain. The light absorption was read by a spectrophotometer (SpectraMax plus 348 microplate reader, Molecular Devices) at 570 nm (ref. 58). The entire experiment was repeated independently.

FA resistance. To test the ability of M6 wild-type or *EwfR::Tn5* to resist FA, the strains were allowed to grow on LB agar medium supplemented with different concentrations of FA (0.01, 0.05 and 0.1%, catalogue no. F6513, Sigma Aldrich).

c-di-GMP chemical complementation. To test if the Tn5 insertion in the predicted guanylate cyclase gene could be complemented by exogenous c-di-GMP, M6 wild-type or *EwgC::Tn5* strains were grown on LB agar medium supplemented with c-di-GMP (0.01 or 0.02 mg ml^{-1}) (catalogue no. TLRL-CDG, Cedarlane). After 24 h, the agar diffusion method was used to test for antifungal activity.

Colicin V assay. To verify that the Tn5 insertion in the predicted colicin V production gene caused loss of colicin V secretion, M6 wild-type or *EwvC*-4B9::Tn5 strains were inoculated as liquid cultures (OD_{600} = 0.5) into holes created in LB agar medium pre-inoculated after cooling with an *E.coli* strain sensitive to colicin V (MC4100, ATCC 35695)[59].

Biochemical and enzymatic assays

Detection of antifungal phenazine derivatives. For phenazine detection, bio-guided fractionation combined with Liquid chromatography-mass spectrometry (LC-MS) analysis was undertaken. Wild-type M6 or mutant bacterial strains were grown for 48 h on Katznelson and Lochhead liquid medium[60], collected by freeze drying, then the lyophilized powder from each strain was extracted by methanol. The methanolic extracts were tested for anti-*Fusarium* activity using the agar diffusion method as described above. The extracts were dried under vacuum and dissolved in a mixture of water and acetonitrile then fractionized over a preparative HPLC C18 column (Nova-Pak HR C18 Prep Column, 6 µm, 60 Å, 25 × 100 mm prepack cartridge, part no. WAT038510, serial no. 0042143081sp, Waters). The solvent system consisted of purified water (Nanopure) and acetonitrile (starting at 99:1 and ending at 0:100) pumped at a rate of 5 ml min^{-1}. The eluted peaks were tested for anti-*Fusarium* activity. Active fractions were subjected to LC-MS analysis. Each of the active fractions was run on a Luna C18 column (Phenomenex) with a gradient of 0.1% formic acid in water and 0.1% formic acid in acetonitrile. Peaks were analysed by mass spectroscopy (Agilent 6340 Ion Trap), electrospray ionization, positive ion mode. LC-MS analysis was conducted at the Mass Spectroscopy Facility, McMaster University.

Gas chromatography-mass spectrometry (GC-MS) to detect production of 2,3-butanediol. To detect 2,3-butanediol, wild-type M6 was grown for 48 h on LB medium. The culture filtrate was analysed by GC-MS (Mass Spectroscopy Facility, McMaster University) and the resulting peaks were analysed by searches against the NIST 2008 database.

Chitinase assay. Chitinase activity of wild-type M6 and the putative chitinase Tn5 mutant was assessed using a standard spectrophotometric assay using the Chitinase Assay Kit (catalogue no. CS0980, Sigma Aldrich) according to the manufacturer's protocol. There were three biological replicates for each culture, and the entire experiment was repeated independently.

Data availability. 16 rRNA sequences for strains M1–M7 have been deposited in GenBank under accession numbers KU307449–KU307455, respectively. Strain M6 DNA sequences have been deposited in GenBank under genome accession number JRJC00000000.1 and at the European Nucleotide Archive under accession number PRJEB7722.

Received 2 March 2016; accepted 10 August 2016; published 26 September 2016

References

1. Goron, T. L. & Raizada, M. N. Genetic diversity and genomic resources available for the small millet crops to accelerate a New Green Revolution. *Front. Plant Sci.* **6,** 157 (2015).
2. Thilakarathna, M. S. & Raizada, M. N. A review of nutrient management studies involving finger millet in the semi-arid tropics of Asia and Africa. *Agronomy* **5,** 262–290 (2015).
3. Hilu, K. W. & de Wet, J. M. J. Domestication of *Eleusine coracana*. *Econ. Bot.* **30,** 199–208 (1976).
4. Mousa, W. K. *et al.* An endophytic fungus isolated from finger millet (*Eleusine coracana*) produces anti-fungal natural products. *Front. Microbiol.* **6,** 1157 (2015).
5. Sundaramari, P. V. A. M. Rationality and adoption of indigenous cultivation practices of finger millet (*Eleusine coracana* (L.) Gaertn.) by the tribal farmers of Tamil Nadu. *Intl. J. Manag. Social Sci.* **2,** 970–977 (2015).
6. Sutton, J. C. Epidemiology of wheat head blight and maize ear rot caused by *Fusarium graminearum*. *Can. J. Plant Pathol.* **4,** 195–209 (1982).
7. Mousa, W. K., Shearer, C., Limay-Rios, V., Zhou, T. & Raizada, M. N. Bacterial endophytes from wild maize suppress *Fusarium graminearum* in modern maize and inhibit mycotoxin accumulation. *Front. Plant Sci.* **6,** 805 (2015).
8. Munimbazi, C. & Bullerman, L. B. Molds and mycotoxins in foods from Burundi. *J. Food Prot.* **59,** 869–875 (1996).
9. Chandrashekar, A. & Satyanarayana, K. Disease and pest resistance in grains of sorghum and millets. *J. Cereal Sci.* **44,** 287–304 (2006).
10. Siwela, M., Taylor, J., de Milliano, W. A. & Duodu, K. G. Influence of phenolics in finger millet on grain and malt fungal load, and malt quality. *Food Chem.* **121,** 443–449 (2010).
11. Wilson, D. Endophyte: the evolution of a term, and clarification of its use and definition. *Oikos* **73,** 274–276 (1995).
12. Johnston-Monje, D. & Raizada, M. N. Conservation and diversity of seed associated endophytes in across boundaries of evolution, ethnography and ecology. *PLoS ONE* **6,** e20396 (2011).
13. Waller, F. *et al.* The endophytic fungus *Piriformospora indica* reprograms barley to salt-stress tolerance, disease resistance, and higher yield. *Proc. Natl Acad. Sci. USA* **102,** 13386–13391 (2005).
14. Haas, D. & Defago, G. Biological control of soil-borne pathogens by fluorescent pseudomonads. *Nat. Rev. Microbiol.* **3,** 307–319 (2005).
15. Mousa, W. K. & Raizada, M. N. The diversity of anti-microbial secondary metabolites produced by fungal endophytes: an interdisciplinary perspective. *Front. Microbiol.* **4,** 65 (2013).
16. Mousa, W. K. & Raizada, M. N. Biodiversity of genes encoding anti-microbial traits within plant associated microbes. *Front. Plant Sci.* **6,** 231 (2015).
17. O'Donnell, K. *et al.* Phylogenetic analyses of RPB1 and RPB2 support a middle Cretaceous origin for a clade comprising all agriculturally and medically important fusaria. *Fungal Genet. Biol.* **52,** 20–31 (2013).
18. Saleh, A. A., Esele, J., Logrieco, A., Ritieni, A. & Leslie, J. F. *Fusarium verticillioides* from finger millet in Uganda. *Food Addit. Contam.* **29,** 1762–1769 (2012).
19. Pall, B. & Lakhani, J. Seed mycoflora of ragi, *Eleusine coracana* (L.) *Gaertn. Res. Develop. Rep.* **8,** 78–79 (1991).
20. Amata, R. *et al.* An emended description of *Fusarium brevicatenulatum* and *F. pseudoanthophilum* based on isolates recovered from millet in Kenya. *Fungal Divers.* **43,** 11–25 (2010).
21. Penugonda, S., Girisham, S. & Reddy, S. Elaboration of mycotoxins by seed-borne fungi of finger millet (*Eleusine coracana* L.). *Int. J. Biotech. Mol. Biol. Res.* **1,** 62–64 (2010).
22. Ramana, M. V., Nayaka, S. C., Balakrishna, K., Murali, H. & Batra, H. A novel PCR–DNA probe for the detection of fumonisin-producing *Fusarium* species from major food crops grown in southern India. *Mycology* **3,** 167–174 (2012).

23. Adipala, E. Seed-borne fungi of finger millet. *E. Afr. Agricult. Forest. J.* **57,** 173–176 (1992).
24. Ettinger, C. L., Mousa, W. M., Raizada, M. N. & Eisen, J. A. Draft genome sequence of *Enterobacter* sp. strain UCD-UG_FMILLET (Phylum Proteobacteria). *Genome Announc.* **3,** e0146-14 (2015).
25. Chongo, G. *et al.* Reaction of seedling roots of 14 crop species to *Fusarium graminearum* from wheat heads. *Can. J. Plant Pathol.* **23,** 132–137 (2001).
26. Pitts, R. J., Cernac, A. & Estelle, M. Auxin and ethylene promote root hair elongation in Arabidopsis. *Plant J.* **16,** 553–560 (1998).
27. Parsons, J. F. *et al.* Structure and function of the phenazine biosynthesis protein PhzF from *Pseudomonas fluorescens* 2-79. *Biochemistry* **43,** 12427–12435 (2004).
28. Lu, J. *et al.* LysR family transcriptional regulator PqsR as repressor of pyoluteorin biosynthesis and activator of phenazine-1-carboxylic acid biosynthesis in *Pseudomonas* sp. M18. *J. Biotechnol.* **143,** 1–9 (2009).
29. Goethals, K., Van Montagu, M. & Holsters, M. Conserved motifs in a divergent nod box of *Azorhizobium caulinodans* ORS571 reveal a common structure in promoters regulated by LysR-type proteins. *Proc. Natl Acad. Sci. USA* **89,** 1646–1650 (1992).
30. Wang, Y., Luo, Q., Zhang, X. & Wang, W. Isolation and purification of a modified phenazine, griseoluteic acid, produced by *Streptomyces griseoluteus* P510. *Res. Microbiol.* **162,** 311–319 (2011).
31. Nakamura, S., Wang, E. L., Murase, M., Maeda, K. & Umezawa, H. Structure of griseolutein A. *J. Antibiot. (Tokyo)* **12,** 55–58 (1959).
32. Giddens, S. R., Feng, Y. & Mahanty, H. K. Characterization of a novel phenazine antibiotic gene cluster in *Erwinia herbicola* Eh1087. *Mol. Microbiol.* **45,** 769–783 (2002).
33. Kitahara, M. *et al.* Saphenamycin, a novel antibiotic from a strain of *Streptomyces*. *J. Antibiot. (Tokyo)* **35,** 1412–1414 (1982).
34. Toyoda, H., Katsuragi, K., Tamai, T. & Ouchi, S. DNA Sequence of genes for detoxification of fusaric acid, a wilt-inducing agent produced by *Fusarium* species. *J. Phytopathol.* **133,** 265–277 (1991).
35. Utsumi, R. *et al.* Molecular cloning and characterization of the fusaric acid-resistance gene from *Pseudomonas cepacia*. *Agric. Biol. Chem.* **55,** 1913–1918 (1991).
36. Marre, M., Vergani, P. & Albergoni, F. Relationship between fusaric acid uptake and its binding to cell structures by leaves of *Egeria densa* and its toxic effects on membrane permeability and respiration. *Physiol. Mol. Plant Pathol.* **42,** 141–157 (1993).
37. Bacon, C., Hinton, D. & Hinton, A. Growth-inhibiting effects of concentrations of fusaric acid on the growth of *Bacillus mojavensis* and other biocontrol *Bacillus* species. *J. Appl. Microbiol.* **100,** 185–194 (2006).
38. Borges-Walmsley, M., McKeegan, K. & Walmsley, A. Structure and function of efflux pumps that confer resistance to drugs. *Biochem. J.* **376,** 313–338 (2003).
39. Hu, R.-M., Liao, S.-T., Huang, C.-C., Huang, Y.-W. & Yang, T.-C. An inducible fusaric acid tripartite efflux pump contributes to the fusaric acid resistance in *Stenotrophomonas maltophilia*. *PLoS ONE* **7,** e51053 (2012).
40. van Rij, E. T., Girard, G., Lugtenberg, B. J. & Bloemberg, G. V. Influence of fusaric acid on phenazine-1-carboxamide synthesis and gene expression of *Pseudomonas chlororaphis* strain PCL1391. *Microbiology* **151,** 2805–2814 (2005).
41. Römling, U., Galperin, M. Y. & Gomelsky, M. Cyclic di-GMP: the first 25 years of a universal bacterial second messenger. *Microbiol. Mol. Biol. Rev.* **77,** 1–52 (2013).
42. Fath, M., Mahanty, H. & Kolter, R. Characterization of a purF operon mutation which affects colicin V production. *J. Bacteriol.* **171,** 3158–3161 (1989).
43. Fath, M. J., Zhang, L. H., Rush, J. & Kolter, R. Purification and characterization of colicin V from *Escherichia coli* culture supernatants. *Biochemistry* **33,** 6911–6917 (1994).
44. Soliman, S. S. *et al.* An endophyte constructs fungicide-containing extracellular barriers for its host plant. *Curr. Biol.* **25,** 2570–2576 (2015).
45. Lee, R. D.-W. & Cho, H.-T. Auxin, the organizer of the hormonal/environmental signals for root hair growth. *Front. Plant Sci.* **4,** 448 (2013).
46. Oldroyd, G. E. Speak, friend, and enter: signalling systems that promote beneficial symbiotic associations in plants. *Nat. Rev. Microbiol.* **11,** 252–263 (2013).
47. Cortes-Barco, A., Hsiang, T. & Goodwin, P. Induced systemic resistance against three foliar diseases of *Agrostis stolonifera* by (2R, 3R)-butanediol or an isoparaffin mixture. *Ann. Appl. Biol.* **157,** 179–189 (2010).
48. Soliman, S. S. & Raizada, M. N. Interactions between co-habitating fungi elicit synthesis of taxol from an endophytic fungus in host *Taxus* plants. *Front. Microbiol.* **4,** 3 (2013).
49. Dereeper, A. *et al.* Phylogeny.fr: robust phylogenetic analysis for the non-specialist. *Nucleic Acids Res.* **36,** 465–469 (2008).
50. Dereeper, A., Audic, S., Claverie, J.-M. & Blanc, G. BLAST-explorer helps you building datasets for phylogenetic analysis. *BMC Evol. Biol.* **10,** 8 (2010).
51. Wang, K., Kang, L., Anand, A., Lazarovits, G. & Mysore, K. S. Monitoring *in planta* bacterial infection at both cellular and whole-plant levels using the green fluorescent protein variant GFPuv. *New Phytol.* **174,** 212–223 (2007).
52. Bric, J. M., Bostock, R. M. & Silverstone, S. E. Rapid *in situ* assay for indoleacetic acid production by bacteria immobilized on a nitrocellulose membrane. *Appl. Environ. Microbiol.* **57,** 535–538 (1991).
53. Shehata, H. *Molecular and Physiological Mechanisms Underlying the Antifungal and Nutrient Acquisition Activities of Beneficial Microbes PhD thesis*, Univ. Guelph (2016).
54. Gaudin, A. C. M., McClymont, S. A., Holmes, B. M., Lyons, E. & Raizada, M. N. Novel temporal, fine-scale and growth variation phenotypes in roots of adult-stage maize (Zea mays L.) in response to low nitrogen stress. *Plant Cell Environ.* **34,** 2122–2137 (2011).
55. Schmale, D. & Bergstrom, G. Fusarium head blight in wheat. *The Plant Health Instructor* **612**, http://dx.doi.org/10.1094/PHI-I-2003-0612-01 (2003).
56. Solovyev, V. & Salamov, A. in *Metagenomics and its Applications in Agriculture, Biomedicine and Environmental Studies* (ed. Li, R. W.) 61–78 (Nova Science, 2011).
57. de Jong, A., Pietersma, H., Cordes, M., Kuipers, O. P. & Kok, J. PePPER: a webserver for prediction of prokaryote promoter elements and regulons. *BMC Genomics* **13,** 299 (2012).
58. Stepanović, S., Vuković, D., Dakić, I., Savić, B. & Švabić-Vlahović, M. A modified microtiter-plate test for quantification of staphylococcal biofilm formation. *J. Microbiol. Methods* **40,** 175–179 (2000).
59. Gérard, F., Pradel, N. & Wu, L.-F. Bactericidal activity of colicin V is mediated by an inner membrane protein, SdaC, of *Escherichia coli*. *J. Bacteriol.* **187,** 1945–1950 (2005).
60. Paulus, H. & Gray, E. The biosynthesis of polymyxin B by growing cultures of *Bacillus polymyxa*. *J. Biol. Chem.* **239,** 865–871 (1964).

Acknowledgements

The authors thank M. Struder-Kypke (Department of Molecular and Cellular Biology, University of Guelph) for assistance with confocal microscopy and for her comments. The authors thank A. Schaafsma and L. Tamburic-Ilincic (Ridgetown College, University of Guelph) for providing hybrid maize and wheat seeds, respectively. The authors also thank M. Atalla for assistance with disease scoring. W.K.M. was supported by generous scholarships from the Government of Egypt and the University of Guelph (International Graduate Student Scholarships, 2012, 2014). The authors thank L. Smith (University of Guelph) for graphics. This research was supported by grants to M.N.R. by the Ontario Ministry of Agriculture, Food and Rural Affairs (OMAFRA), Grain Farmers of Ontario (GFO), the Natural Sciences and Engineering Research Council of Canada (NSERC) and the CIFSRF programme, jointly funded by the International Development Research Centre (IDRC, Ottawa) and Global Affairs Canada.

Author contributions

W.K.M. designed and conducted all experiments, analysed all data and wrote the manuscript. C.S. assisted in greenhouse trials. V.L.-R. performed the DON quantification experiments. C.L.E. and J.A.E. sequenced the M6 genome and provided gene annotations. M.N.R. helped to design the experiments and edited the manuscript. All authors read and approved the manuscript.

Additional information

Supplementary information is available for this paper. Reprints and permissions information is available at www.nature.com/reprints. Correspondence and requests for materials should be addressed to M.N.R.

Competing interests

The authors declare no competing financial interests. However, a provisional US patent has now been filed on the application of M6 to corn and wheat (US patent application no. 62/056,012).